Thermal stress and pore pressure development in microwave heated concrete

A. Akbarnezhad* and K.C.G. Ong[a]

*Department of Civil Engineering, National University of Singapore, # 04-03E,
Block E2, 5 Engineering drive 2, Singapore 117576*

Abstract. Most previous studies have generally overlooked the contribution of thermal stresses generated within the concrete mass when subjected to microwave heating and reported on pore-pressure as being the dominant cause of surface spalling. Also, the variation in electromagnetic properties of concrete and its effects on the microwave heating process have not been studied in detail. In this paper, finite element modeling is used to examine the simultaneous development of compressive thermal stresses and pore-pressure arising from the microwave heating of concrete. A modified Lambert's Law formulation is proposed to estimate the microwave power dissipation in the concrete mass. Moreover, the effects of frequency and concrete water content on the concrete heating rate and pattern are investigated. Results show high compressive stresses being generated especially in concrete with a high water content when heated by microwaves of higher frequencies. The results also reveal that the water content of concrete plays a crucial role in the microwave heating process.

Keywords: concrete; microwaves; contamination; heating; thermal stress; pore pressure.

1. Introduction

Microwave heating of concrete has applications in various fields of civil engineering. These applications usually take advantage of the capabilities of a range of microwave frequency targeted to heat the concrete to different extents and degree of uniformity. Microwave heating at low frequencies, such as 915 MHz, can be used to heat the concrete uniformly. One example of uniform microwave heating applications is the microwave curing of prefabricated concrete components.

On the other hand, it is well known that microwaves of higher frequencies can generate high temperature gradients inside the concrete, occurring between the microwave exposed surface and the cooler interior. Such non-uniform heating in a very short time duration leads to a high differential temperature gradient and thus high thermal stresses. Moreover, concrete is a material whose pores may be partially filled by water and air. Under ambient temperature condition, part of the water is chemically bonded to the cement (non-evaporable water) while the remainder is contained in the concrete pores as free (evaporable) water. The free water includes both the capillary water and the gel water which resides partially within the hydrated product. When exposed to microwaves, as a result of dielectric losses, microwaves penetrating the concrete act as a volumetrically distributed heat source. The free water in the concrete is a very strong dipole and is easily heated up, as it

---

* Corresponding author, E-mail: ceeaa@nus.edu.sg
[a] E-mail: ceeongkc@nus.edu.sg

absorbs the microwave energy. As a result, the free water within the concrete evaporates. When the evaporation rate overtakes the vapor migration rate, pore pressure builds up. The two phenomena of thermal stresses and pore pressure have been postulated to cause delamination of the concrete surface layer when exposed to high power microwave heating. Although undesirable when uniform microwave heating is required (e.g. in microwave curing of concrete), the thermal stresses and pore pressure developed may be harnessed as a demolition tool to cause spalling of the heated concrete surface layer.

One application of this is on concrete that has been used for structural and shielding purposes in nuclear power plants and nuclear waste processing plants. As a consequence of long-term usage various radionuclides diffuse into the concrete, contaminating the surface layer. The thickness of the contaminated layer depends on the concrete diffusivity and exposure duration and is usually between 1 to 10 mm (0.039 to 0.39 inch) (Spalding 2000). Microwave heating has been recently considered as a potential replacement for conventional methods of concrete surface decontamination. This method not only increases the efficiency of the decontamination process but also eliminates some of the drawbacks such as dust generation, health hazards, etc.

Microwave decontamination of the concrete's surface has also recently found applications in the recycling of concrete, utilizing the process to remove the physical and chemical contaminants from the surface of the concrete debris (Ayers 1998, Akbarnezhad *et al.* 2011). Available literature shows that the existence of non-concrete impurities (contaminants) in the concrete debris are one of the main causes of the lower quality of the recycled concrete aggregate (RCA) compared to the natural aggregate (Ayers 1998). Currently the decontamination process is done manually which is too energy consuming and inefficient. Due to its higher rate compared to the conventional techniques, microwave decontamination can be used to increase the quality and yield of the RCA production plants. In this paper, the capability of microwave heating to remove the contaminated surface layer of concrete is numerically examined.

2. Literature review

"Concrete breaking by microwaves" first appeared as the subject of an experimental study in UK by Watson in 1968. Over the years, several research groups including the Japan's Atomic Energy Research Institute (JAERI), UK's Harwell Laboratory and US's Oak Ridge National Laboratory (ORNL) (White *et al.* 1992, 1995) tried to develop methods and the necessary machinery to use microwave as demolition tool to remove radioactive wastes from the surfaces of concrete. Besides the experimental efforts, a few analytical studies have focused on modeling the microwave heating phenomenon to correlate to the experimental observations (Lagos *et al.* 1995). Li *et al.* (1993, 1994) examined the pore pressure and temperature distribution within a concrete sample with variable dielectric properties when exposed to microwaves of frequencies 0.896, 2.45, 10.6 and 18 GHz. However, none of the earlier studies reported in available literature seemed to take into account the thermal stresses arising from the high temperature gradient. In a recent publication, (Zi and Bažant 2003, Bažant and Zi 2003) used the finite volume method to determine temperature and pore pressure development as well as thermal stresses in the heated zone. However the effects of moisture condition of the concrete and microwave frequency on the concrete dielectric properties were not taken into consideration in full.

3. Main causes of concrete surface spalling

Available literature suggests two hypotheses dealing with the delamination phenomenon. The first adheres closely to studies on the effects of fire on the pore water pressure generated within the concrete mass. Modeling of heat and mass transfer seemed to suggest generation of the pore water pressure within the concrete in excess of the concrete tensile strength (Li *et al*. 1993, Lagos *et al*. 1995). The other hypothesis initiated by Zi and Bažant (2003), Bažant and Zi (2003), postulates that stresses generated by a differential thermal gradient play a more significant role in the decontamination process. The thermal expansion of the saturated heated zone resisted by the colder surrounding concrete mass, leads to very high compressive stresses parallel to the surface which either crush the concrete, or cause the surface layer to buckle or both. Moreover, since the porosity of a typical concrete is around 0.1, the actual pore pressures generated are only about a tenth of those predicted by the other researchers and does not seem sufficient to cause spalling (Zi and Bažant 2003). Bažant *et al*. also claimed that the effect of pore pressure would in fact be even weaker because of the additional pore space created by the formation of microcracks.

4. Research significance and objectives

There is significant ambiguity concerning the main cause of concrete surface spalling when subjected to microwave heating. Moreover, the significant effects of concrete water content and microwave frequency on the electromagnetic properties of concrete and thus on the concrete heating rate and pattern have been overlooked in available literature. On the other hand, the methods commonly used to model microwave power dissipation in concrete are not easy to use and include many mathematical and electromagnetic modeling complexities.

In this paper, the COMSOL Mutiphysics finite element software is used to numerically study the relative contribution of thermal stresses and pore-pressure in the delamination of the concrete's surface when subjected to microwave heating at different frequencies. The simple approximate method proposed in this study can be easily used to estimate the microwave power dissipation in concrete without dealing with the mathematical complexities of accurate electromagnetic analysis. Moreover, this study is aimed at illustrating the significant effect of concrete water content on the magnitude and pattern of the stresses developed. Furthermore, the variation of concrete EM properties with frequency and its effect on developing stresses are examined.

5. Estimation of the microwave power dissipation in concrete

5.1 Microwaves

Microwaves are a portion of the electromagnetic spectrum lying between UHF (ultrahigh frequency) radio waves and heat (infrared) waves and span the frequency range of 300 MHz-300 GHz. In order to gain an insight into the phenomena which leads to the heat generation in a material exposed to microwave, a detailed knowledge of the electric and magnetic fields together with an understanding of the dielectric behavior of the material is necessary. Generally, regardless of the selected numerical scheme, Maxwell's equations are used to describe the behavior of microwaves. They govern

radiation propagation in a dielectric medium. For source-free problems, the differential form of the Maxwell's equation can be expressed in terms of the electric field intensity E and the magnetic field intensity H (Pozar 1998)

$$\nabla \times E = -\frac{\partial(\mu H)}{\partial t}, \ \nabla \times H = \sigma E + \frac{\partial(\varepsilon H)}{\partial t}, \ \nabla \cdot (\varepsilon E) = 0, \ \text{and} \ \nabla . H = 0 \tag{1}$$

Where, σ is the electrical conductivity, t is time, ε is the permittivity, and μ is the permeability. Once the electric field intensity is obtained from Maxwell's equations, the locally dissipated power can be evaluated using the Poynting theorem.

5.2 Dielectric properties

Every material has a unique set of electromagnetic properties affecting the way in which the material interacts with the electric and the magnetic waves. Concrete is a dielectric (nonmetallic) material. A dielectric material can be characterized by two independent electromagnetic properties, the complex permittivity ε and the complex (magnetic) permeability μ (Rhim and Buyukozturk 1998). Complex permittivity is defined as

$$\varepsilon = \varepsilon' - i\varepsilon'' \tag{2}$$

Where, ε' is the real part of complex permittivity and ε'' is the imaginary part of complex permittivity. Dividing this by the permittivity of the free space, ε_0, the property becomes dimensionless and relative to the permittivity of the free space

$$\frac{\varepsilon}{\varepsilon_0} = \frac{\varepsilon'}{\varepsilon_0} - i\frac{\varepsilon''}{\varepsilon_0} \tag{3}$$

Or,

$$\varepsilon_r = \varepsilon_r' - i\varepsilon_r'' \tag{4}$$

Where, ε_0 is the permittivity of the free space, ε_r is the relative permittivity, ε_r' is the dielectric constant and ε_r'' is the loss factor of the material. Dielectric constant is a measure of how much energy from an external electric field is stored in a material and the loss factor is a measure of how dissipative or lossy a material is to an external field (Rhim and Buyukozturk 1998).

5.3 Reflection and transmission of the waves at the air-concrete interface

The mismatch between the dielectric constants at the interface between two different media causes some of the incident waves to be reflected and the rest to be transmitted into the next medium. Mathematical expression of the reflected wave can be written as

$$R = \frac{\sqrt{\varepsilon_{r2}}\cos\theta_i - \sqrt{\varepsilon_{r1}}\cos\theta_t}{\sqrt{\varepsilon_{r2}}\cos\theta_i + \sqrt{\varepsilon_{r1}}\cos\theta_t} \tag{5}$$

Where, R is the reflection coefficient, ε_{r1} is the dielectric constant for medium 1 (air), ε_{r2} is the dielectric constant for medium 2 (concrete), θ_i is the angle of incidence and θ_t is the angle of transmission (Fig. 1). The square of reflection ($\left|R^2\right|$) is called reflectivity and denoted as r. The transmissivity, C_T, is obtained from:
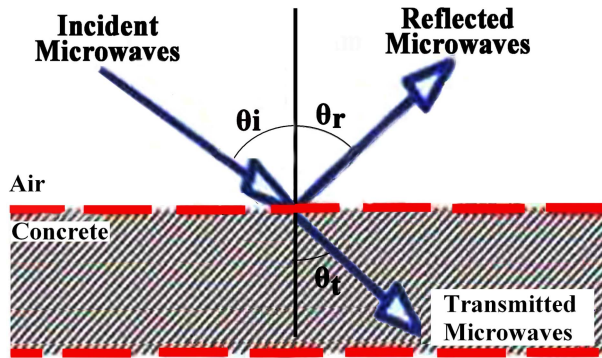
Fig. 1 Reflection and transmission of the waves at the air-concrete interface

$$C_T = 1 - r \tag{6}$$

5.4 Effect of water content and microwave frequency on dielectric properties

The amount of the energy dissipated in concrete varies dramatically with its electromagnetic properties. Electromagnetic properties of concrete are a function of factors such as concrete ingredients and mix proportions, water content, microwave frequency, temperature, etc. However, despite the significant effect of concrete water content and the microwave frequency on the heating process, they have not been fully considered in previous studies. Li and Ebadian (1994) considered frequency and temperature dependence of the dielectric properties of concrete without reporting on the effects of concrete water content. Bažant and Zi (2003) assumed that the volume fraction of water of the concrete in nuclear facilities is about 7% and seemed to have ignored the dependence of the electromagnetic properties of concrete on the incident microwave frequency. It is noteworthy that throughout this paper, the water content is referring to the concrete's evaporable water content including both the capillary and gel water.

In this paper, in order to study the significance of water content, four different types of concrete specimens are considered: (1) wet specimen, standing water on its surface, (2) saturated, surface dry concrete, (3) air-dried concrete exposed to ambient room temperature and humidity, (4) oven-dried concrete with zero moisture content by weight. In addition, the variation in dielectric properties with microwave frequency is taken into account in estimating the power dissipation.

5.5 Microwave power dissipation

The power flux associated with a propagating electromagnetic wave is represented by the Poynting vector S and the time average flux for the harmonic fields is given by

$$S = \frac{1}{2} E \times H^* \tag{7}$$

Where,* denotes the complex conjugate. According to the Poynting theorem the power dissipation in the medium is

$$\oint_s S.nds = -\frac{1}{2}\omega\varepsilon_0\varepsilon_r'' \int_v E.E^* dv + i\omega\int_v \left(\frac{\mu_0}{2}H.H^* + \frac{\varepsilon_0\varepsilon_r'}{2}E.E^*\right)dv \tag{8}$$

which states that the net power flow across a surface S enclosing a volume V equates to the power dissipated in the medium (real part), and that stored in the electric and magnetic fields (imaginary part). Applying the divergence theorem to Eq. (8), the point form of Poynting theorem is

$$\nabla . S = -\frac{1}{2} \omega \varepsilon_0 \varepsilon_r'' \, E.E^* + i\omega \left(\frac{\mu_0}{2} H.H^* + \frac{\varepsilon_0 \varepsilon_r'}{2} E.E^* \right) \tag{9}$$

Hence, the power dissipated per unit volume can be written as

$$P^M(r) = -Re(\nabla . S) = \frac{1}{2} \omega \varepsilon_0 \varepsilon_r'' \, |E|^2 \tag{10}$$

As illustrated above, Maxwell's equations can be used to describe any microwave problem. However, owing to their complex formulation, approximations are usually used to predict the electromagnetic wave behavior in materials. The most common approximation is Lambert's Law which considers an exponential decay of microwave energy absorption inside the medium. Ayappa *et al.* (1991), compared numerical model predictions using Maxwell and Lambert's law to represent power dissipation in slabs. They obtained a critical thickness above which the use of Lambert's approximation is valid and showed that the two formulations predict identical power profiles for slabs at least 2.7 times thicker than the penetration depth. Similar results were reported by Barringer *et al.* (1995) comparing predictions by the individual and combined models during heating of gel samples.

5.6 Lambert's law

If I is the transmitted power flux into the medium, then the variation $I(x)$ with distance x from the sample surface is

$$I(x) = I_0 e^{-2\beta x} \tag{11}$$

Where, I_0 is the incident power and β is the attenuation factor for a given material and frequency

$$\beta = \frac{2\pi f}{c} \sqrt{\frac{\varepsilon_r' \left(\sqrt{1 + \left(\frac{\varepsilon_r''}{\varepsilon_r'} \right)} - 1 \right)}{2}} \tag{12}$$

Here, c is the speed of light and f is the microwave frequency. Hence, the power absorbed per unit volume at distance x, $PL(x)$, may be estimated as (Ayappa *et al.* 1991)

$$PL(x) = -\frac{\partial I(x)}{\partial x} = 2\beta I_0 e^{-2\beta x} \tag{13}$$

The use of Lambert's law requires an estimate of the transmitted power intensity I_0, which can be obtained from calorimetric measurements (Ohlsson and Bengtsson 1971, Taoukis *et al.* 1987) or used as an adjustable parameter to match experimental temperature profiles with model predictions (Nykvist and Decareau 1976). Alternatively, as adopted in this study, if I_0 is the incident power flux, then Lambert's law must be modified to account for the decrease in power due to reflection at the surface of the concrete sample. In this paper, the transmissivity coefficient, C_T, is applied to account for the reflected microwave energy
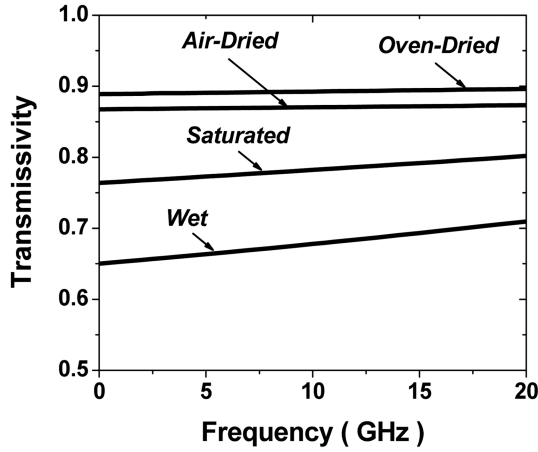
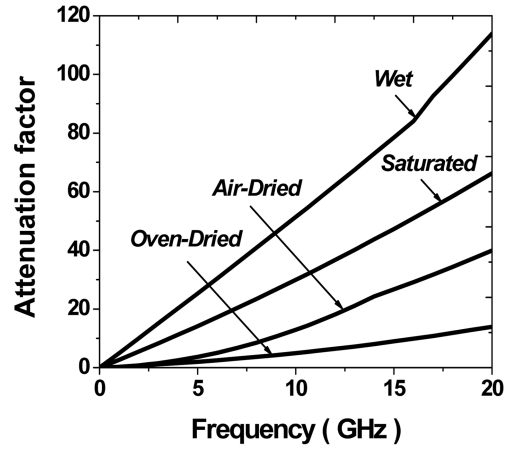Fig. 2 The transmissivity of concrete at different moisture conditions and microwave frequencies

Fig. 3 The attenuation factor of concrete at different moisture conditions and microwave frequencies

$$PL(x) = -\frac{\partial I(x)}{\partial x} \times C_T = 2\beta I_0 e^{-2\beta x} \times C_T \tag{14}$$

The transmissivity coefficients and attenuation factors for concrete specimens with different moisture contents and at different frequencies were calculated using the data from Rhim and Buyukozturk (1998) and are illustrated in Figs. 2 and 3. It is noteworthy that the dielectric constants and loss factors as reported in Rhim and Buyukozturk (1998) are considerably higher than similar values assumed by Bažant and Zi (2003), and Li and Ebadian (1994).

5.7 Modification for microwave modes

In practice, a hollow metallic tube either of rectangular or circular cross section, made of aluminum, copper, or brass of various sizes is usually used to transmit the generated microwave. Such a structure is commonly known as a waveguide.

In previous studies, the incident power has been postulated to be uniformly distributed in the transverse plane. However, this is not the case in practice. The fundamental transverse electric and transverse magnetic modes, TE_{10} and TM_{11}, are usually excited in the waveguides. The Transverse electric mode TE_{10} is the usual choice for the single-mode commercial waveguides. It does not vary in one of the transverse directions while having a sinusoidal distribution in the other. Hence, it represents a similar heating problem to that of heating a two dimensional slab. In this study, Eq. (14) is modified to account for the sinusoidal shape of the TE_{10} mode.

The incident TE_{10} mode has the form of $E = (0,0,E_z) = \{0,0,\sin[\pi(a-y)/2a]\}$; where, $2a$ is the width of the waveguide. However, as can be seen in Eq. (10), the dissipated energy is proportional to the square of the electric field's norm. Therefore, it seems quite reasonable to consider a sine^2 shape to simulate the TE_{10} mode with the approximate Lambert's Law.

$$I(x) = P \sin^2\left(\pi\frac{a-y}{2a}\right) \times e^{-2\beta x} \tag{15}$$

The sine^2-shape incident power equivalent to uniform power I_0 in Eq. (14) may be computed as

$$2aI_0 = 2 \times \int_0^a P\sin^2\left(\pi\frac{a-y}{2a}\right) \Rightarrow P = 2I_0 \tag{16}$$

Hence, the final power dissipation function may be written as

$$PL(x) = -\frac{\partial I(x)}{\partial x} \times C_T = 2\beta \times (2I_0) \times e^{-2\beta x} \times C_T \times Sin^2\left(\pi\frac{a-y}{2a}\right) \tag{17}$$

Comparing Eq. (17) to Eq. (14) illustrates that the incident microwave power delivered through a TE_{10} mode waveguide has a peak incident power that is twice the equivalent uniform incident power adopted by most previous studies (Li *et al.* 1993, Li and Ebadian 1994, Zi and Bažant 2003, Bažant and Zi 2003).

6. Problem description

In this paper, pore pressure and thermal stresses developed in the heated zone of a large concrete block subjected to microwave radiation through a waveguide applicator are numerically computed. A possible sketch of a typical microwave decontamination system is shown in Fig. 4. To guarantee the accuracy of Lambert's Law, the concrete block is assumed to be thick enough to be treated as infinitely thick to microwave radiation. According to Ayappa *et al.* (1991), this is the case when the sample is at least 2.7 times thicker than the penetration depth d_p of microwave power. The power penetration depth is defined as the depth $1/e$ at which the transmitted power drops to of its initial value at the surface and is calculated by (Saltiel and Datta 1999)
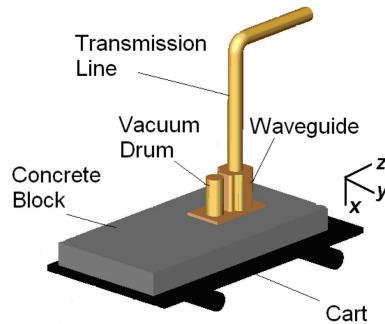

Fig. 4 Sketch of the microwave decontamination system

Table 1 The minimum thickness of concrete block to guarantee the validity of Lambert's Law (Estimation of the actual microwave penetration depth in concrete)

Frequency (GHz)	Moisture condition			
	Wet	Saturated	Air-dried	Oven-dried
	Minimum thickness of concrete block, cm, (in.)			
2.45	10.96 (4.31)	19.97 (7.86)	122.53 (48.24)	161.30 (63.50)
10.6	2.47 (0.97)	4.23 (1.66)	9.40 (3.70)	25.09 (9.88)
18	1.36 (0.53)	2.31 (0.91)	3.93 (1.55)	11.40 (4.49)

Table 2 Standard waveguide dimensions at different frequencies

Microwave frequency (GHz)	Designation	Width, mm (in.)	Height, mm (in.)
2.45	WR340	86.36 (3.4)	43.18 (1.7)
10.6	WR90	22.86 (0.9)	10.16 (0.4)
18	WR42	10.66 (0.42)	4.31 (0.17)

$$d_p = \frac{1}{2\beta} = \frac{c}{2\sqrt{2}\,\pi f \sqrt{\varepsilon'}\,[\sqrt{1+\tan^2\delta}-1\,]^{1/2}} \tag{18}$$

Here, β is the attenuation factor of the material. Table 1 lists the abovementioned minimum thickness for the concrete blocks considered in this study. The area of the heated zone depends on the waveguide dimensions which vary with frequency as shown in Table 2. Dimensions of the concrete block are assumed to be large enough in comparison with the heated zone dimensions to ignore electromagnetic scattering and provide structural constraint around the heated zone.

7. Formulation

In general, the microwave decontamination problem involves solving Maxwell's equations which govern the propagation of microwave radiation through the material and microwave waveguide or cavity, the heat transfer equation which governs the heat absorption and the resulting temperature rise in the concrete block, and the mass transfer equation which governs the pore pressure development in the concrete block. However, due to the complexities of Maxwell's equations, the modified Lambert's Law (Eq. (17)) is used to estimate the microwave power dissipation in concrete.

7.1 Heat transfer and thermal stress analyses

Having the microwave power dissipation estimated, the heat transfer equation can be formulated as

$$\rho C_H \frac{\partial T}{\partial t} = -\nabla.(-K\nabla T) + PL(x) \tag{19}$$

Here, ρ = mass density of concrete, t = time, ∇ = gradient operator, C_H = specific heat of concrete, K = heat conductivity and T = temperature.

As the next step, the temperature distribution obtained from Eq. (19) is used as the input data for the thermal stress analysis.

7.2 Mass transfer

The mass conservation equation for this problem may be written as

$$\frac{\partial w}{\partial t} + \nabla.J = HD(w) \tag{20}$$

Here, w = specific water content, t = time, ∇ = gradient operator, J = water flux vector, and $HD(w)$ = change in free water content because of hydration and dehydration. The water flux J can be expressed in

terms of the gradient of pore pressure (Bažant and Zi 2003)

$$J = -\frac{a}{g}\nabla P \tag{21}$$

Where, P = the pore pressure, a = permeability, and g = gravity acceleration. The free water content in the liquid phase within the concrete can be determined by means of the so-called 'Equation of state of pore pressure' (Bažant and Kaplan 1996). For temperatures above the critical point of water (374.15°C), all free water is assumed to have been vaporized and thus there is no liquid phase. For temperatures below the critical point of water, the free water content was found to depend on temperature and the ratio of water vapor pressure to saturation vapor pressure. In this study, the semi-empirical expressions from Bažant and Kaplan (1996) are used. For nonsaturated concrete the following formula has been proposed

$$\frac{w}{C} = \left(\frac{W_{s1}}{C} \times h\right)^{\frac{1}{m(T)}} \quad h \leq 0.96 \tag{22}$$

Here, w is the water content of concrete, w_{s1} is the saturation water content at 25°C, C is the mass of (anhydrous) cement per m^3 of concrete, $h = P/(P_s(T))$ where $P_s(T)$ = saturation pore pressure at temperature T, and $m(T)$ is an experimentally determined empirical expression as follows (Bažant and Kaplan 1996)

$$m(T) = 1.04 - \frac{(T+10)^2}{22.3(25+10)^2 + (T+10)^2} \tag{23}$$

For saturated concrete, the free water-to-cement ratio is determined by Bažant and Kaplan (1996)

$$\frac{w}{C} = \frac{w_{s1}}{C}[1 + 0.12(h - 1.04)] \quad h \geq 1.04 \tag{24}$$

In this study, the transition between $h = 0.96$ and $h = 1.04$ is assumed to be a straight line joining the $w_{0.96}$ value $w_{1.04}$ and; Thus

$$w = w_{h=0.96} + (h - 0.96) \times \frac{w_{h=1.04} - w_{h=0.96}}{1.04 - 0.96} \quad 0.96 \leq h \leq 1.04 \tag{25}$$

The saturation pore pressure at different temperatures can be calculated using the following semi-empirical equation (Rei *et al.* (1987))

$$Ln\left(\frac{P_s}{P_c}\right) = \frac{T_c}{\overline{T}}[a(1 - T_r) + b(1 - T_r)^{1.5} + c(1 - T_r)^3 + d(1 - T_r)^6] \tag{26}$$

Where, $\overline{T}$ is the absolute temperature (in Kelvin), $T_r = T/T_c$, $T_c = 647.7K$, $P_c = 22.07\ MPa$, $a = -7.7654$, $b = 1.45938$, $c = -2.7758$ and $d = -1.23303$.

At ambient temperatures the permeability of concrete is controlled by nanopores, which explains the extremely low permeability at these temperatures. But this is not the case at high temperatures. When the temperature is increased above 100°C, the permeability increases sharply. This can be explained by heat-induced changes in the structure of small pores. The following expressions have been proposed by Bažant and Thonguthai (1978) to predict the variation of permeability with temperature

$$a = a_0 f_1(h) f_2(T) \quad \text{for} \quad T \le 100^\circ\text{C}$$

and

$$a = a_0 f_2(100) f_3(T) \quad \text{for} \quad T > 100^\circ\text{C}$$

(27)

Where, a_0 = Reference permeability at $T = 25^\circ\text{C}$ and, $f_1(h), f_2(T), f_3(T)$ are functions described by following expressions

$$f_1(h) = \alpha + \frac{1-\alpha}{1 + \left(\dfrac{1-h}{1+h_c}\right)^4} \quad \text{for} \quad h \le 1; \text{ and } f_1(h) = 1 \text{ for } h \ge 1$$

(28)

Here, $\alpha = 1 / [1 + 0.253(100 - \min(T, 100^\circ\text{C}))]$ and, $h_c = 0.75$

$$f_2(T) = \exp\left[\frac{Q}{R}\left(\frac{1}{T_0} - \frac{1}{T}\right)\right]$$

(29)

$$f_3(T) = 5.5\left\{\frac{2}{a + \exp[-0.455(T-100)]} - 1\right\} + 1$$

(30)

Where, Q = activation energy for water migration, $\overline{T_0} = 298^\circ\text{K}$ and R = gas constant. Having taken the above into consideration, the pore pressure and the moisture distribution in the concrete specimen can then be obtained by coupling Eqs. (19) and (20).

7.3 Heat and mass transfer boundary conditions

At the boundaries with ambient air and surrounding unheated concrete, both conductive and radiative heat losses occur. Hence, the heat transfer boundary condition may be written as

$$\nabla T.n + B_i(T - T_a) + S(T^4 - T_a) = 0$$

(31)

Where B_i is the Biot number, a measure of relative effect of convective heat loss compared to thermal conduction, S is the radiation number, a measure of relative effect of radiative heat loss compared to thermal conduction, n is the normal to the boundary and T_a is the ambient temperature. For a small heat-loss limit (B_i, $S \rightarrow 0$), a zero heat flux boundary condition results; while for the large heat-loss limit (B_i, $S \rightarrow \infty$), a fixed-temperature boundary condition is obtained. Similarly, for mass transfer the following boundary condition is imposed

$$J.n + B_w(P_a - P) = 0$$

(32)

Where, P_a is the ambient pressure, P is the vapor pressure at the surface, and B_w is the moisture transfer coefficient which may vary from 0 for a sealed surface to ∞ for the case of free air convection near the concrete surface. In this paper a sealed concrete surface is considered.

8. Results and discussions

The commercially available COMSOL Multiphysics finite element software is used to solve the coupled mass transfer, heat transfer and structural problem explained. The equation-based modeling

module of COMSOL Multiphysics can be used to solve the general form of differential equations and PDE's for the defined model. In this study, the general form equation module was used to perform the mass transfer analysis formulated. The effect of different parameters, such as variation of concrete porosity and saturation pore pressure with temperature, were taken into account using the Matlab codes which can be simultaneously run through COMSOL Multiphysics' Matlab interface. Finally, structural and heat transfer modules were coupled with the general form equation module and solved simultaneously to account for the coupling effects in this multiphysics problem.

The mechanical and thermal properties of concrete used in this numerical study are summarized in Table 3. Since the results for all frequencies would be too numerous and to make it possible to compare the results obtained with the results reported in available literature, the frequencies of 2.45, 10.6 and 18 GHz are considered. These three frequencies are representative of the characteristics of typical low, intermediate and high frequencies used in microwave heating. Moreover, a constant incident microwave power of 1.1 MW/m^2 is considered. Because microwave heating at higher frequencies generally leads to a faster temperature rise within the concrete specimen, different heating durations of 5, 2 and 1 seconds were chosen for heating at frequencies of 2.45, 10.6 and 18 GHz, respectively. The heating durations chosen resulted in magnitudes of thermal stresses

Table 3 Mechanical and thermal properties of concrete

| Property	Assumption	Unit
Density	2300 (143.58)	Kg/m^2, (lb/ft^3)
Specific heat	1000 (0.24)	$J[Kg^oK]$, $(Btu/[lb.^oF])$
Thermal conductivity	3 (1.73)	$W/[m.K]$, $(Btu/[ft.hr.^oF])$
Thermal expansion coefficient	12×10^{-6} (6.67×10^{-6})	$1/^oC$, $(1/^oF)$
Heat transfer coefficient of heat flux	10.0 (1.76)	$W[m^2.^oK]$, $(Btu/[ft^2.hr.^oF])$
Modulus of elasticity	48.5 (7034.33)	GPa, (ksi)
Poisson's ratio	0.12	
Surface emissivity	0.9	
Initial temperature	25 (77)	^oC, (^oF)
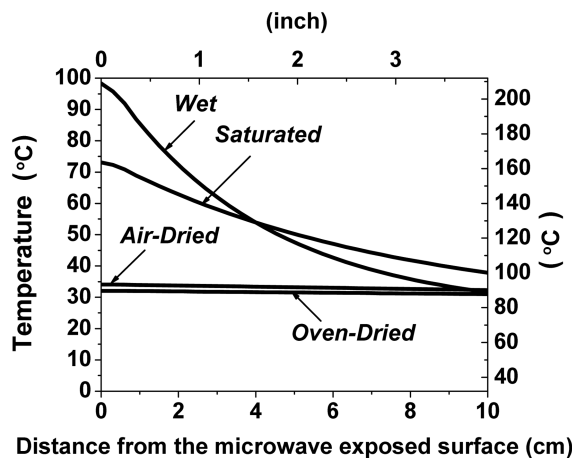
Fig. 5 Temperature distribution in concrete after 5 seconds of microwave heating at 2.45 GHz frequency
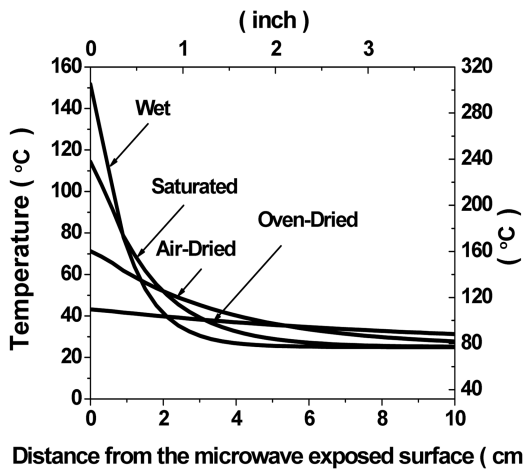
Fig. 6 Temperature distribution in concrete after 2 seconds of microwave heating at 10.6 GHz frequency
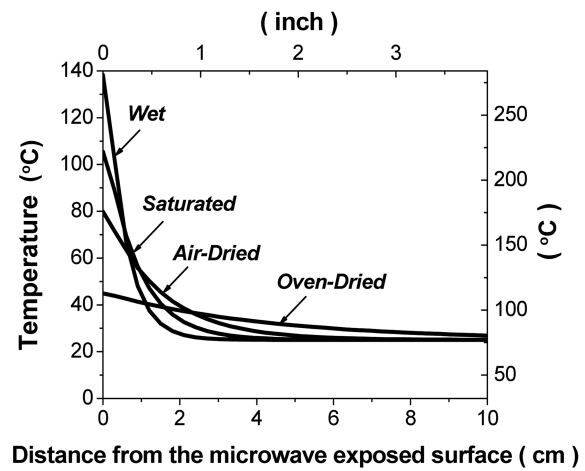
Fig. 7 Temperature distribution in concrete after 1 second of microwave heating at 18 GHz frequency

developed that would be meaningful when benchmarked against the respective strength of concrete. To increase the legibility of figures, the variation of results within the first 10 cm thick surface layer of the concrete blocks is illustrated.

8.1 Temperature distribution

Temperature distribution in the microwave heated concrete and its variation with microwave frequency and the concrete's water content are plotted in Figs. 5 to 7. As expected, the temperature distribution patterns at different frequencies and different water contents of concrete resemble the approximate microwave power dissipation pattern and decay exponentially.

As can be seen in Figs. 5 to 7, for a microwave power of 1.1 MW/m^2, at higher frequencies and higher water contents, microwave penetration is reduced and more energy is dissipated near the concrete surface. This results in higher temperature rise and temperature gradients within a thin surface layer of the concrete sample.

Results can be easily explained by considering the variation of the concrete's EM properties with the microwave frequency and the concrete's water content. As can be seen in Fig. 3, the attenuation factor (β) of concrete increases with the concrete's water content and the microwave frequency. On the other hand, as can be deduced from Eq. (18), the microwave power penetration depth is reduced by an increase in the concrete attenuation factor. The lesser the penetration of the microwave power the more energy is dissipated in a thinner surface layer of concrete. Therefore, an increase in the concrete's water content and/or the microwave frequency leads to a decrease in the microwave penetration depth and hence more energy is dissipated in a thinner surface layer of concrete. This results in a higher temperature rise and thermal gradient.

On the contrary, as can be seen in Figs. 5 to 7, a reduction in the concrete's water content and/or the microwave frequency can significantly decrease the microwave heating rate and hence microwave power decay inside the concrete. As can be seen in Fig. 5, both the heating rate and power dissipation rate have been significantly reduced for the air-dried and oven-dried concretes so
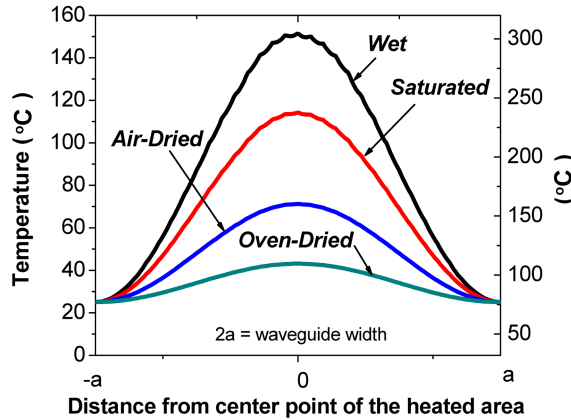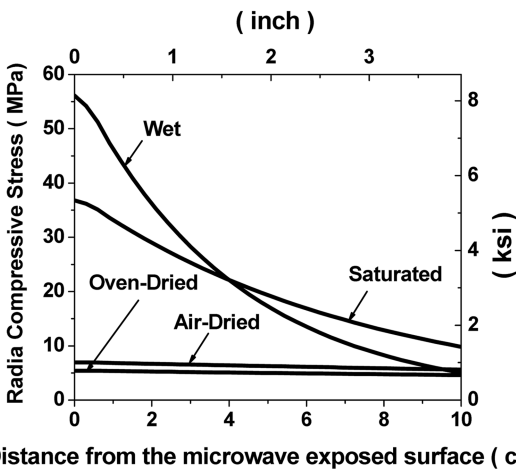
Fig. 8 Temperature distribution across the microwave exposed surface of concrete after 2 seconds of microwave heating at 10.6 GHz frequency

that they are heated in an almost uniform pattern and at a very slow heating rate.

In addition, the temperature profile across the microwave exposed surface of concrete for heating at a frequency of 10.6 GHz is plotted in Fig. 8. As can be seen, the sinusoidal shape of the TE_{10} microwave mode resulted in a sinusoidal temperature rise across the exposed surface of concrete.

8.2 Thermal stresses

Temperature gradient in the heated zone of concrete results in nonuniform expansion of this area and may develop relatively high compressive stresses. The results of the thermal stress analysis for different microwave frequencies and the concrete's water contents are shown in Figs. 9 to 11. Moreover, the stress developed across the microwave exposed surface of concrete is plotted in Fig.

Fig. 9 Radial compressive stress in concrete after 5 seconds of microwave heating at 2.45 GHz frequency
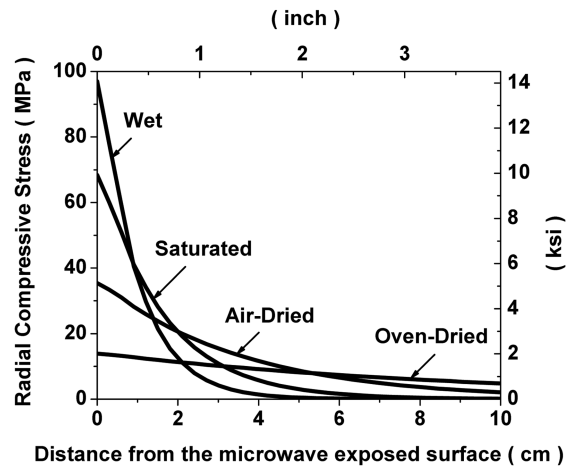
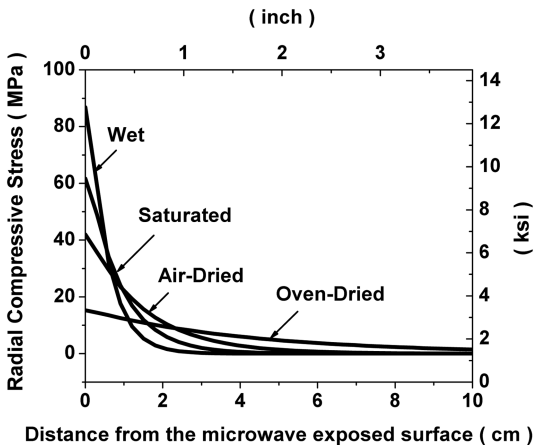Fig. 10 Radial compressive stress in concrete after 2 seconds of microwave heating at 10.6 GHz frequency

Fig. 11 Radial compressive stress in concrete after 1 second of microwave heating at 18 GHz frequency
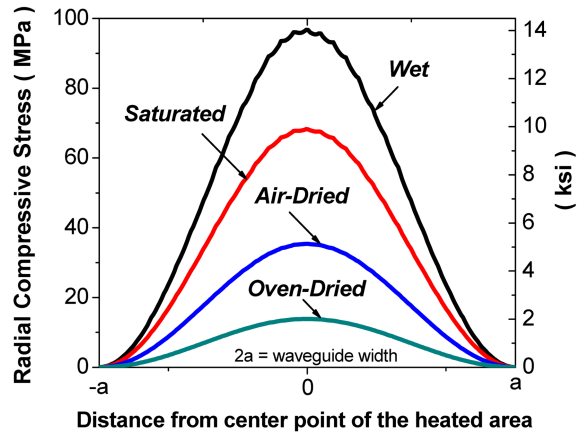
Fig. 12 Radial compressive stress distribution across the microwave exposed surface of concrete after 2 seconds of microwave heating at 10.6 GHz frequency

12. Such plots may be of use when choosing the appropriate microwave specifications for a given nominal strength and depth of spalling. Similarly, for a specific microwave power, microwave frequency and concrete's water content, the approximate spalling depth can be easily estimated. As can be seen, just after a few seconds of microwave heating, especially at high frequencies and water contents, considerably high compressive stresses may develop. The radial compressive stress developed may crush the concrete surface layer when it exceeds the concrete's compressive strength. Hence, the results confirm the capability of high frequency microwaves to remove the surface layer of concrete through development of a localized field of high thermal stresses.

8.3 Pore pressure

The pore pressure development in saturated concrete specimens subjected to microwave at different frequencies is illustrated in Figs. 13 and 14. As can be seen, the pore pressure variation with the microwave frequency and the concrete's water content shows a similar pattern as explained for temperature and thermal stress effects. Pore pressure may lead to concrete surface spalling when the stresses generated exceed the concrete's tensile strength. Comparing the values of pore pressure obtained to the compressive thermal stresses developed for similar cases of microwave exposure serves to highlight the prominent role that the thermal stresses play in spalling of the concrete surface. Nevertheless, considering the inherent weakness of concrete in tension, the contribution of pore pressure should also be considered in the predictions.

8.4 Effect of water content

According to Eq. (14), the microwave energy dissipation in any material depends on its attenuation factor and transmissivity values. Moreover, these two factors vary with microwave frequency and the water content of the concrete. The significant effect of the water content of concrete on the magnitude and pattern of stress development has been demonstrated in Figs. 5 to
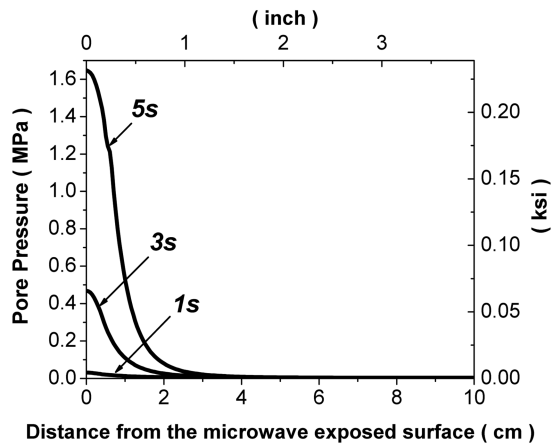
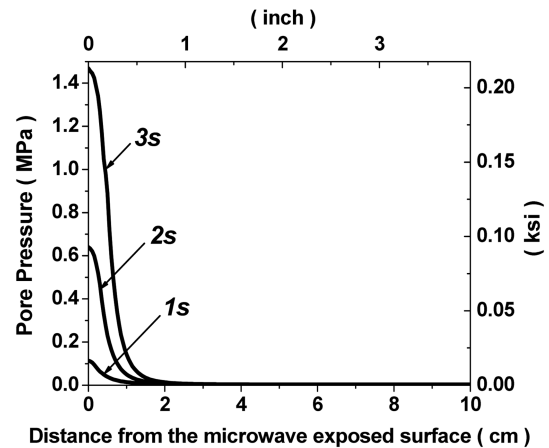Fig. 13 Pore pressure in saturated concrete after 5 seconds of microwave heating at 10.6 GHz frequency

Fig. 14 Pore pressure in saturated concrete after 3 seconds of microwave heating at 18 GHz frequency

12. As can be seen, higher water content leads to faster and more concentrated stress development in the heated specimen which speeds up the surface delamination process. In practice, most of the contaminated concrete blocks are old and most likely to be in an air-dried condition; hence, drenching the concrete surface may be used as an appropriate method both to speed up the process and control the spalling depth.

8.5 Effect of microwave frequency

As explained in section 8.1, in general, for a given microwave power and heating period, higher microwave frequencies result in a faster temperature rise within a thinner surface layer of concrete. Therefore, higher stresses and pore pressure are generated within the surface layer of concrete. The thickness of the concrete surface layer heated may be explained by the microwave penetration depth. The theoretical microwave penetration depth (as defined in Section 6) for heating at a given microwave frequency and concrete moisture content may be calculated by replacing the respective attenuation factor in Eq. (18) with those from Fig. 3. However, a more realistic approximation of the actual penetration depth of microwaves at different frequencies may be obtained by using the minimum thicknesses of the concrete slab as recommended by Ayappa *et al.* (1991). These are listed in Table 1.

The effect of microwave frequency on the maximum thermal stresses generated in concrete specimens with different water contents is shown in Fig. 15. As can be seen, an increase in microwave frequency can lead to significantly higher compressive stresses.

8.6 Comparison with the available literature

To compare the results obtained in this study with those from available literature, the maximum temperatures predicted using the proposed method are compared with the results of the most reliable previous study conducted by Zi and Bažant (2003), Bažant and Zi (2003). These results are depicted in Figs. 16 and 17. As mentioned earlier, it seems that the variation of the concrete's electromagnetic properties with the concrete's water content and the microwave frequency has been overlooked in previous
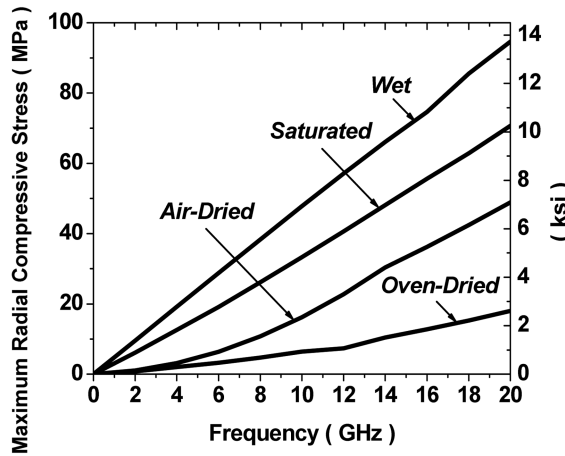
Fig. 15 The variation of maximum compressive stress in concrete with frequency after 1 second of microwave heating
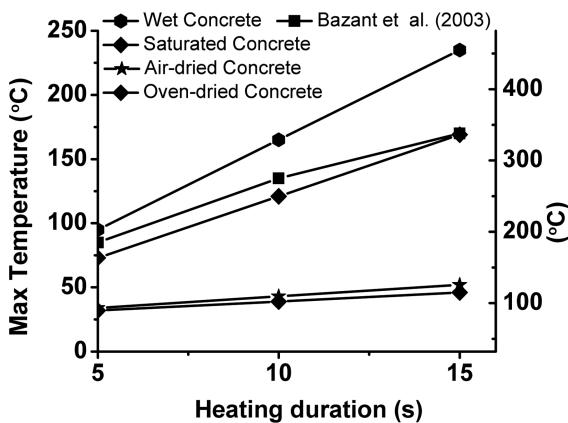

Fig. 16 Comparison between the maximum temperatures in concrete obtained in this study and the results reported by Bažant *et al.* at the same microwave frequency of 2.45 GHz and microwave incident power of 1.1 MW/m²
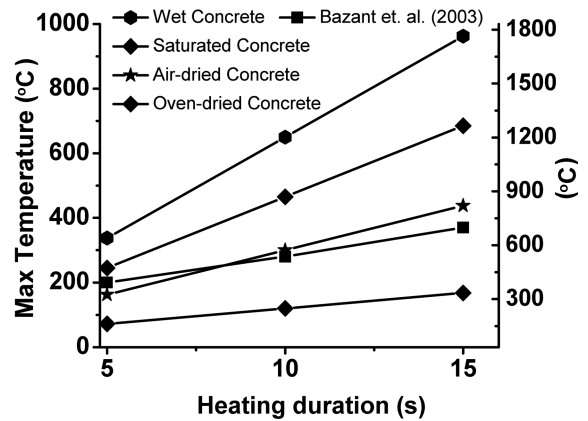

Fig. 17 Comparison between the maximum temperatures in concrete obtained in this study and the results reported by Bažant *et al.* at the same microwave frequency of 10.6 GHz and microwave incident power of 1.1 MW/m²

studies. All the previous studies have considered constant electromagnetic properties at all the microwave frequencies investigated. This wrong assumption will significantly affect the accuracy of the results. To illustrate this, the results are compared at two different frequencies of 2.45 and 10.6 GHz.

To make the comparison more sensible, results of the current study (as shown in Figs. 16 and 17) were re-calculated under the similar conditions (i.e. similar incident microwave power, incident power distribution and boundary conditions) to those used in Bažant *et al.*'s study. As can be seen in Figs. 16 and 17, the results reported by Bažant *et al.*'s study are roughly in agreement with the results obtained in this study. At 2.45 GHz, the temperatures reported by Bažant *et al.* locate in between the results obtained for the saturated concrete and the wet concrete while at 10.6 GHz they almost resemble the results obtained for the air-dried concrete. This shows that the relative

magnitude of temperatures reported by Bažant *et al.* to those obtained in this study decreases with an increase in the microwave frequency. This decrease stems from the fact that the loss factor of concrete increases with the frequency (Fig. 3) which will lead to higher temperature rise. However, the variation of dielectric properties of concrete with the microwave frequency was not considered by Bažant *et al.*

9. Conclusions

1. The well known Lambert's Law approximate method was modified to account for the TE_{10} microwave mode used in common microwave heating systems and the reflections at the concrete surface. This method can be easily used to predict the microwave power dissipation in concrete while avoiding the mathematical complexities of accurate electromagnetic modeling using Maxwell's equations.

2. The results confirm the capability of high frequency microwaves to remove the surface layer of concrete by developing a localized field of both high thermal stresses and pore pressure.

3. The results of finite elements analysis confirm the prominent role that thermal stresses play in concrete surface spalling, as first highlighted by Bažant *et al.* (2003).

4. Drenching of the concrete surface with copious amount of water may be used to increase the efficiency of the microwave decontamination process, as considerably higher stresses in a thinner surface layer (Table 1) may be generated.

5. The results reveal the high sensitivity of the microwave heating process to the water content of concrete. Therefore, prior to any analytical or experimental investigation, the water content of concrete and its corresponding electromagnetic properties should be measured.

6. The spalling depth of the concrete surface layer and the time for spalling to occur are inversely proportional to the microwave frequency.

References

Akbarnezhad, A., Ong, K.C.G., Zhang, M.H., Tam, C.T. and Foo, T.W.J. (2011), "Microwave-assisted beneficiation of recycled concrete aggregates", *Constr. Build. Mater.*, **25**, 3469-3479.

Ayappa, K.G., Davis, H.T., Crapiste, G., Davis, E.A. and Gordon, J. (1991), "Microwave heating: an evaluation of power formulations", *Chem. Eng. Sci.*, **64**(4), 1005-1016.

Ayers, K.W. (1998), *Feasibility of recycling contaminated concrete,* Environmental Engineering, Vanderbilt University, Nashville, Tennessee, United States.

Barringer, S.A., Davis, E.A., Gordon, J., Ayappa, K.G. and Davis, H.T. (1995), "Microwave heating temperature profiles for thin slabs compared to Maxwell and Lambert's law predictions", *J. Food Sci.*, **60**(5), 1137-1142.

Bažant, Z.P. and Goangseup, Zi. (2003), "Decontamination of radionuclides from concrete by microwave heating. I: Theory", *J. Eng Mech.*, **129**(7),777-784.

Bažant, Z.P. and Kaplan, M.F. (1996), C*oncrete at high temperatures: material properties and mathematical models*, Harlow, Essex: Longman Group.

Bažant, Z.P. and Thonguthai, W. (1978), "Pore pressure and drying of concrete at high temperature", *J. Eng. Mech. Div. - ASCE*, **104**(5), 1059-1079.

Lagos, L.E., Li, W. and Ebadian, M.A. (1995), "Heat transfer within a concrete slab with a finite microwave heating source", *Int. J. Heat Mass Tran.*, **38**(5), 887-897.

Li, W. and Ebadian, M.A. (1994), "Heat and mass transfer in a contaminated porous concrete slab with variable

dielectric properties", *Int. J. Heat Mass Tran.*, **37**(6), 1013-1027.

Li, W., Ebadian, M.A., White, T.L. and Grubb, R.G. (1993), "Heat transfer within a concrete slab applying the microwave decontamination process", *J. Heat Transfer*, **115**(1), 42-50.

Nykvist, W.E. and Decareau, R.V. (1976), "Microwave meat roasting", *J. Microwave Power*, **11**(1), 3-24.

Ohlsson, T. and Bengtsson, N. (1971), "Microwave heating profiles in foods-a comparison between heating experiments and computer simulation", *Microw. Energy Appl. Newsl.*, **4**(6), 3-8.

Pozar, D.M. (1998), *Microwave engineering*, John Wiley & Sons.

Rei, R.C., Prauznitz, J.M. and Poling, R.E. (1987), *The properties of gases and liquids*, 4th Ed., McGraw Hill, New York.

Rhim, H.C. and Buyukozturk, O. (1998), "Electromagnetic properties of concrete at microwave frequency range", *J. ACI Mater.*, **95**(3), 262-271.

Saltiel, G. and Datta, A.K. (1999), "Heat and mass transfer in microwave processing", *Adv. Heat Trans.*, **33**(1), 91-94.

Spalding, B. (2000), "Volatility and extractability of Strontium-85, Cesium-134, Cobalt-57, and Uranium after heating hardened portland cement paste", *Env. Sci. Tech.*, **34**(23), 5051-5058.

Taoukis, P., Davis, E.A., Davis, H.T., Gordon, J. and Talmon, Y. (1987), "Mathematical modeling of microwave thawing by the modified isotherm migration method", *J. Food Sci.*, **52**(2), 455-463.

Watson, A. (1968), *Breaking of concrete*, Microwave power engineering, E.C. Okress, ed, Vol. 2, Academic, New York.

White, T.L., Foster, D. Jr., Wilson, C.T. and Schaich, C.R. (1995), *Phase II: microwave concrete decontamination results*, ORNL Rep. No. DE-AC05-84OR21400., Oak Ridge National Laboratory, Oak Ridge, Tenn.

White, T.L., Grubb, R.G., Pugh L.P., Foster, D. Jr. and Box, W.D. (1992), "Removal of contaminated concrete surface by microwave heating - Phase 1 results", *Proceedings of 18th American Nuclear Society Symposium on Waste Management,* Tucson, AZ., American Nuclear Society, La Grange Park, Illinois, 745-748.

Zi, Goangseup and Bažant, Z.P. (2003), "Decontamination of radionuclides from concrete by microwave heating. II: Computations", *J. Eng Mech.*, **129**(7), 785-792.

CC